HSI Health Sciences Investigations Journal

share

Send us an email: hsijournal@ug.edu.gh
Visit us: https://www.hsijournal.ug.edu.gh

ISSN Online 2704-4890 | ISSN Print 2720-7609

Online first publication

Original Research Article

HSI Journal (2025) Volume 7 (Issue 1):1092-1103. https://doi.org/10.46829/hsijournal.2025.6.7.1.1092-1103

Open Access

Optimised formulation of *Mallotus oppositifolius* extract reverses cognitive decline and beta-amyloid deposition in a murine Alzheimer's disease-like dementia model

James T PEWEE [1], Emmanuel K OFORI [2], Kevin K ADUTWUM-OFOSU [3], Donatus W ADONGO [4], Patrick AMOATENG [5], Ofosua ADI-DAKO [6*], Kennedy KE KUKUIA [1*]

[1]Department of Medical Pharmacology, University of Ghana Medical School, College of Health Sciences, University of Ghana, Accra, Ghana; [2]Department of Chemical Pathology, University of Ghana Medical School, College of Health Sciences, University of Ghana, Accra, Ghana; [3]Department of Anatomy, University of Ghana Medical School, College of Health Sciences, University of Ghana, Accra, Ghana; [4] Department of Pharmacology, School of Pharmacy, University of Health and Allied Sciences, Ho, Ghana; [5] Department of Pharmacology and Toxicology, School of Pharmacy, College of Health Sciences, University of Ghana, Accra, Ghana. [6] Department of Pharmaceutics and Microbiology, School of Pharmacy, College of Health Sciences, University of Ghana, Accra, Ghana

Received December, 2025; Revised May, 2025; Accepted May,2025

Abstract

Background: *Mallotus oppositifolius* leaf extract (MOE) has potential neuroprotective effects, but no scientific investigation validates its use in mouse models of Alzheimer's disease (AD).

Objective: The study evaluated the effects of an optimised formulation of MOE in aluminium chloride ($AlCl_3$)-induced AD-like dementia.

Methods: Mice were randomly assigned to 6 groups (n = 10), and AD was induced in groups 2-6 using $AlCl_3$ (175 mg/kg), with group 1 representing the negative control. Optimised formulation of MOE (10, 30 and 100 mg) was administered orally to groups 3, 4 and 5, respectively, while group 2 represented the disease control. The Morris water maze (MWM) test was used to assess cognitive impairment, and the open-field test (OFT) for locomotor and anxiety behaviour. Biochemical and histological changes were also assessed.

Results: $AlCl_3$ caused significant memory and learning disruption in the MWM test, but MOE formulation (10, 30, and 100 mg/kg) reversed these deficits. MOE formulation attenuated the reduction in both locomotion and time spent in the centre of the OFT in comparison to the $AlCl_3$-diseased untreated group. Brain superoxide dismutase (SOD) content was significantly increased while brain and serum malondialdehyde (MDA), as well as acetylcholinesterase (AChE), were reduced by the formulation treatment when compared to the $AlCl_3$-diseased untreated group. The administration of MOE formulation (30 and 100 mg/kg) resulted in a significant reduction in brain concentrations of IL-1β, IL-6, and TNF-α and a significant decrease in serum IL-6 and TNF-α concentrations when compared to the $AlCl_3$-diseased untreated group. Congo red-stained hippocampus CA1 showed that the formulation (30 and 100 mg/kg) significantly decreased amyloid deposition in comparison to the $AlCl_3$-diseased untreated group.

Conclusion: This study reports that an optimised formulation of MOE improves learning and memory, attenuates anxiety, and reduces pro-inflammatory cytokines and oxidative stress associated with AD-like dementia. The formulation also ameliorates amyloid deposition.

Keywords: *Mallotus oppositifolius*, Alzheimer's disease, β-amyloid, neurodegenerative diseases

Cite the publication as Pewee JT, Ofori EK, Adutwum-Ofosu KK, Adongo DW, Amoateng P et al. (2025) Optimised formulation of *Mallotus oppositifolius* extract reverses cognitive decline and beta-amyloid deposition in a murine Alzheimer's disease-like dementia model. HSI Journal 7 (1): 1092-1103. https://doi.org/10.46829/hsijournal.2025.6.7.1.1092-1103

INTRODUCTION

Alzheimer's disease (AD) has become a global health menace among various neurodegenerative diseases (NDs) due to its debilitating nature [1,2]. The exact cause and associated factors that underlie individual variations regarding the disorder and related symptoms are still unknown [3]. The neurodegeneration associated with AD advances latently and persistently until symptoms such as challenges in memory retention and cognitive abilities that include orientation, problem-solving, and personality changes become evident. AD is distinguished by the

* *Corresponding author*
Email: kkekukuia@ug.edu.gh, oadi-dako@ug.edu.gh

share
Send us an email: hsijournal@ug.edu.gh
Visit us: https://www.hsijournal.ug.edu.gh

presence of extracellular neurofibrillary tangles (NFTs) and intracellular amyloid accumulations [4]. Of these, beta-amyloid (Aβ) and hyperphosphorylated tau (p-tau) are major pathological markers found in AD brain tissues [5,6]. Additional features include mitochondrial dysfunctionality, synaptic destruction, neuroinflammation, dysregulation in neurotransmission, changes in hormonal levels, and dysregulation in the cell cycle [7]. Oxidative stress, a key element in the initiation and progression of AD, is also crucial for the development of Aβ and NFTs [6]. By 2018, dementia, a key AD symptom, had reached a pandemic level, affecting 50 million individuals globally with an estimated yearly economic cost of $1 trillion [8]. Ageing is projected to significantly contribute to a threefold increase in dementia cases by 2050 [8,9]. For most dementia patients, therapeutic options are limited, and there is no effective cure [2]. In this regard, evaluating the therapeutic effects of medicinal plants against dementia may be a viable option.

Mallotus oppositifolius (M. oppositifolius) extract has significant CNS depressant, analgesic, and anticonvulsant effects [10]. It improved spatial memory and learning tasks in mice [11] and reduced MDA levels in liver homogenate tissues of alloxan-induced diabetic rats, suggestive of anti-peroxidative potential [12]. Moreover, many phytochemicals such as diterpenoids, triterpenoids, cardenolides, benzopyrans, flavonoids, coumarinolignoids and phloroglucinol derivatives, (+)-α-tocopherol (vitamin E), lupeol, stigmasterol, phytol, bergenin, squalene, and methyl gallate, and vitamin C with possible beneficial neuroactive effects have been found in the plant [13]. Recently, we reported the presence of methyl laurate, ethyl palmitate, ethyl stearate, benzoic acid derivatives and phenolic compounds in *M. oppositifolius* [14]. Methyl laurate, the most abundant constituent, reduces LPS-induced nuclear factor κ-B levels, while ethyl palmitate, the most abundant fatty acid in the brain, caused a reduction in tumour necrosis factor-α and interleukin-6 in rats [15]. Ethyl stearate blocked α-synuclein in rats, suggesting a possible neuroprotective effect in Parkinson's disease [16]. These pharmacological properties make the plant a viable candidate in managing AD, although this has not been scientifically validated.

Despite these advantages, the effectiveness of plant-based therapies can be limited by poor solubility and instability in gastric and colonic juices, poor absorption, and reduced penetration across the blood-brain barrier [17,18,19]. To address this, the development of novel drug transport systems as carriers for plant extracts can facilitate efficient drug delivery to target sites at an optimal rate. In this regard, chitosan nanoparticles can be used as drug carriers because of their excellent biocompatibility and ease of creating sustained-release formulations [20]. Thus, our study used chitosan nanoparticles to incorporate *M. oppositifolius* leaf extract into a modified-release formulation and evaluated its effect in an AD-like model of dementia.

MATERIALS AND METHODS

Extraction of *M. oppositifolius* leaf extract

M. oppositifolius leaves were obtained from and authenticated at the Centre for Plant Medicine Research (CPMR), Mampong-Akuapem, Ghana. The extraction method followed a similar procedure according to Kukuia et al., 2022 [13]. The air-dried and pulverised leaves underwent cold maceration in 70% ethanol and 30% water for three days. The resultant extract was then concentrated under reduced pressure and at 60°C using a rotary evaporator. The extract was further dried at 45°C, yielding 31.5 g (1.05%) and stored in a desiccator for subsequent use.

Preparation of optimised formulation of *M. oppositifolius*

Formulations of *M. oppositifolius* extract (MOE) were obtained from the Pharmaceutics Lab, School of Pharmacy, University of Ghana. The extraction of pectin from cocoa pod husk [21] and formulation of the oral modified release *Mallotus oppositifolius* multi-particulate matrix were done according to the method used by [22,23,24] with minor modifications. Table 1 shows the proportions used in the formulation of MOE extract in doses of 10, 30, and 100 mg, respectively.

Table 1. Proportions of MOE and excipients in formulation

SN	MOE extract (mg)	Chitosan (mg)	Dicalcium phosphate (mg)	Pectin (mg)	Total weight (mg)
F1(10)	10	50	240	50	350
F1(30)	30	50	220	50	350
F1(100)	100	50	150	50	350

Chemicals

Aluminium chloride ($AlCl_3$) and chitosan were obtained from Central Drug House (India); ketamine hydrochloride from Swiss Parenterals Ltd (India); Sodium phosphate buffer from Thermo Fisher Scientific (USA).

Experimental animals and housing

Institute of Cancer Research (ICR) mice (n = 60) were purchased from the Noguchi Memorial Institute for Medical Research, University of Ghana, and acclimatised for 7 days. Mice aged 24 weeks were grouped in sets of 10 and placed in six stainless cages, each measuring 47 cm × 34 cm × 18 cm (length, width, and height, respectively), containing softwood shavings. Temperature conditions of 25 - 28°C with a 12-hour light/12-hour dark cycle were maintained throughout the study. Mice had unrestricted access to both food and water during the study, except for periods when they were undergoing tests.

Experimental design

A randomised sampling technique was used to group all animals (n = 60). Randomisation was performed by

share
Send us an email: hsijournal@ug.edu.gh
Visit us: https://www.hsijournal.ug.edu.gh

numbering (marking) the animals from 1 to 60. These numbers were entered into Microsoft Excel and randomised into six groups. Induction of AD followed a method similar to that employed by Chen et al. [25] with slight modifications. Group 1 was treated as the vehicle control group (VEH) and was given a regular diet and oral normal saline (0.9%) only. Group 2 was given 175 mg/kg of aluminium chloride by oral route for 25 days to induce AD, followed by administration of 0.9% (5 ml/kg) oral normal saline from the 26th day to the 35th day ($AlCl_3$ group). Groups 3, 4, and 5 received the same dose of $AlCl_3$ as those in group 2 for 25 days, followed by treatment with 10, 30, and 100 mg/kg of optimised MOE for each group, respectively, from the 26th day to the 35th day (+MOE group). Group 6 received the same dose of $AlCl_3$ as those in group 2 for 25 days, followed by administration of 3 mg/kg donepezil from the 26th day to the 35th day as a reference drug group (+DPZ group). While transgenic models offer advantages such as reproducibility, consistency, and genetic relevance to human subjects, the $AlCl_3$ model effectively mimics key features of AD, hence its application in this study.

Morris water maze (MWM) test

The MWM test was used to evaluate the animal's spatial memory and learning. Escape latency and probe memory trials were carried out as they are important for assessing cognitive function in rodent models of neurodegenerative diseases such as AD [26]. The MWM involved a circular pool (1.8 m diameter, 0.4 m height) divided into four quadrants, with a hidden escape platform (0.1 m diameter) in one quadrant. Mice were trained to find the platform within 60 seconds before inducing AD-like dementia. Post-induction, their ability to find the platform was tested to establish a baseline for learning impairment. Treatment with MOE or donepezil (DPZ) started 24 hours later and lasted 10 days. From days 6 to 10, the water level was raised to 0.01 m above the platform, and non-dairy milk was added to obscure it.

Escape latency was recorded to assess spatial learning and memory. During the training trials, each mouse was placed in the pool from different starting positions and allowed to swim for a maximum of 60 seconds to locate the hidden platform. If successful, the time taken to reach the platform was recorded as the escape latency; if unsuccessful, a maximum latency of 60 seconds was assigned, and the mouse was guided to the platform and allowed to remain there for 15 seconds to aid learning. Four trials per day were conducted over the 5-day testing period.

A probe trial was conducted 24 hours after the last test, measuring time spent in the target quadrant without the platform. For the probe trial, the platform was removed, and each mouse was allowed to swim freely for 60 seconds. The amount of time spent in the quadrant where the platform was previously located and the number of times the mouse crossed the former platform location were recorded as measures of spatial memory retention. All observations were made by a blinder.

Open-field (OF) test

The OF locomotion test was employed to examine motor function and to assess anxiety behaviour. The OF was made of a wooden box measuring 100 cm (length) × 100 cm (width) × 25 cm (height). The box was divided into lines of equal distance (20 cm apart). The centre square of the box measured 60 cm (length) × 60 cm (width). In the test, a behavioural tracker was used to assess animal behaviour for 5 minutes. At the beginning of the test, the mouse was positioned in the centre of the open field. Total distance travelled, which was measured by the number of lines crossing, time spent in the centre area, and the frequency of grooming, was evaluated.

Biochemical analysis - Serum collection

Mice were anesthetised with 100 mg/kg ketamine hydrochloride and sacrificed. Blood sample of 0.5 ml was collected from each mouse through cardiac puncture and allowed to clot for 20 minutes. After centrifugating the samples at 4000 rpm for 10 minutes, the serum was obtained and kept at -2^0 0C for measurement of superoxide dismutase (SOD.), malondialdehyde (MDA), acetylcholinesterase (AChE), interleukin-1β (IL-1β), interleukin-6 (IL-6), and tumour necrosis factor-α (TNF-α).

Brain tissue processing

Using sterile instruments, the brain was quickly removed from each mouse's skull after anaesthesia and placed in a pre-chilled dish. The hippocampal, entorhinal, striatum, and cerebral cortex tissues obtained from 6 animals in each group were microdissected, weighed and transferred to microcentrifuge tubes. The brain tissue homogenates of 100 mg/ml were created by adding sodium phosphate buffer (pH of 7.4), using a homogeniser. After homogenisation, the samples were centrifuged at 3500 rpm for 20 minutes at a temperature of 4 °C. The resulting transparent supernatant was obtained and preserved at -20 °C for the measurement of SOD, MDA, AChE, IL-1β, IL-6, and TNF-α.

Determination of biochemical markers

Acetylcholinesterase (AChE) levels, which frequently increase around amyloid plaques and neurofibrillary tangles, are prevalent in AD pathology [28]. Brain and serum AChE, malondialdehyde (MDA), the antioxidant superoxide dismutase (SOD), inflammation-related markers, IL-1β, IL-6 and tumour necrosis factor-α were measured using the sandwich ELISA purchased from the Sunlong Biotech Co., Ltd, China.

Histopathological Analysis

The hippocampal brain tissues were carefully excised from the control and treatment groups (four mice per group), sliced into smaller pieces, and immersed in Bouin's fixative solution for 24 hours. After fixation, the tissues were subjected to paraffinisation and sectioned (5 µm thickness) with a microtome. The sections were stained with Congo red to identify amyloid protein deposits and examined

share
Send us an email: hsijournal@ug.edu.gh
Visit us: https://www.hsijournal.ug.edu.gh

under microscopy. Three (3) micrographs from each group were used for amyloid quantification.

Statistical analysis

GraphPad Prism for Windows version 10.0.2 (GraphPad Software, San Diego, CA, United States) was used for data and statistical analysis. All data were expressed as the mean ± standard error of the mean (SEM). The statistical analysis involved either one-way or two-way analysis of variance (ANOVA), followed by Tukey's post-hoc test. P value < 0.05 among means was considered statistically significant.

RESULTS

Effects of optimised leaf extract of *M. oppositifolius* formulation on $AlCl_3$-induced AD mice by MWM test

Results are shown as time course curves (Figure 1A) and violin plots (Figure 1B, C). In comparison to VEH, $AlCl_3$ treatment increased (F (4,38) = 6.579; p = 0.0003) the latency to locate the platform (escape latency) throughout the experimental period (Figure 1A). Similarly, $AlCl_3$ increased (F (5,58) = 45.65; p < 0.0001) the overall escape latency (depicted as the AUC, Figure 1B) while decreasing

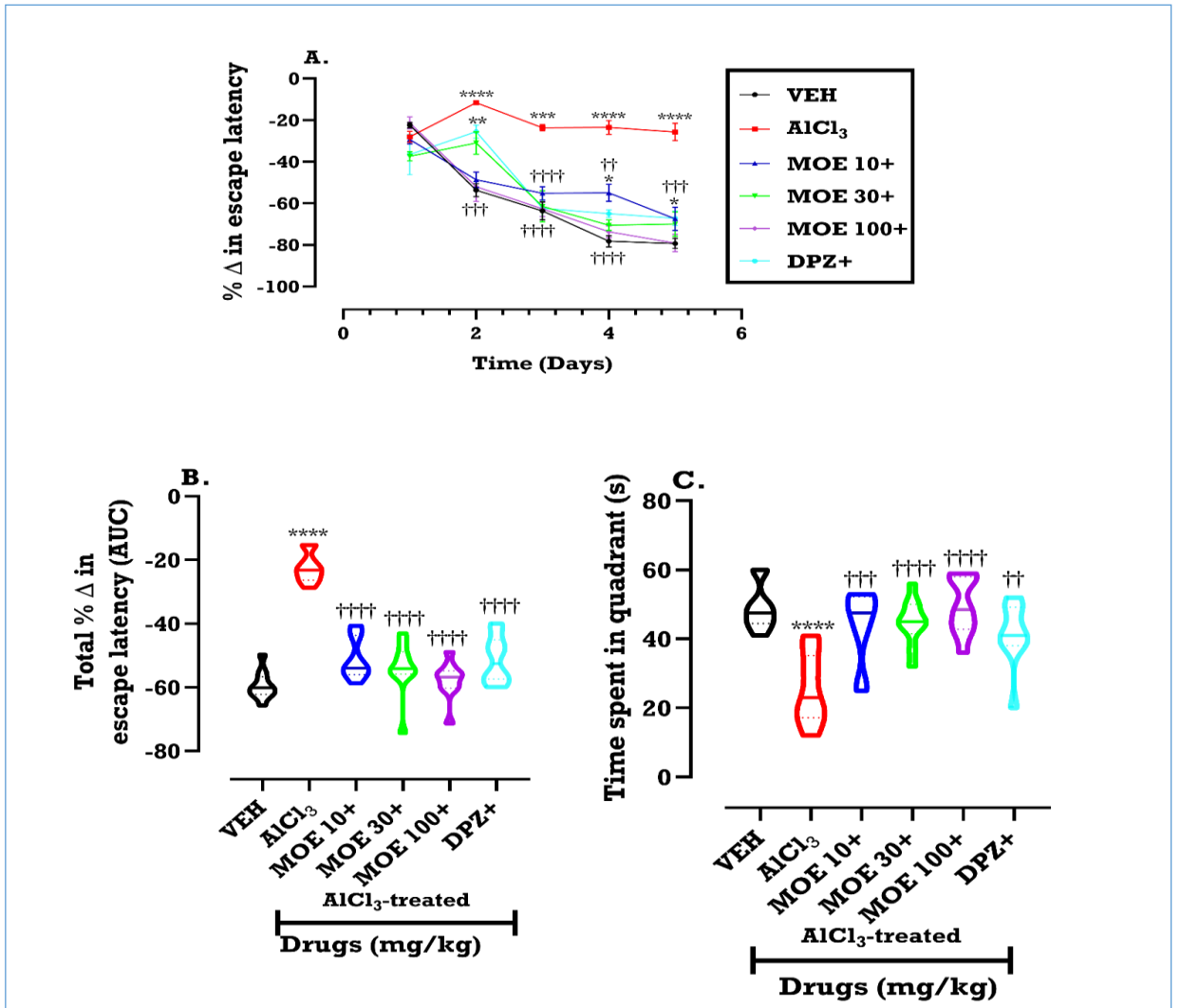

Effects of optimised formulation from the leaf extract of *M. oppositifolius* on $AlCl_3$ induced AD-like dementia in the Morris water maze test (MWT): (A) Percentage change in escape latency; (B) total percentage change in escape latency, calculated as area under the curve (AUC), and (C) Probe memory trial. All data were presented as mean ± SEM (A) time course curve, (B) violin plot of its AUC, and (C) violin plot of its probe memory trail. (A): ****p < 0.0001, ***p < 0.001, **p < 0.01, *p < 0.05; compared to vehicle–control group: (two-way ANOVA followed by Tukey's post hoc test). (B), (C): Significantly different from vehicle-control group (n = 5): ****P < 0.0001: (One way ANOVA followed by Tukey's post hoc test). Significantly different from disease-control ($AlCl_3$) group (n = 5): ††††p < 0.0001, †††p < 0.001, ††p < 0.01: (One way ANOVA followed by Tukey's post-hoc test).

share
Send us an email: hsijournal@ug.edu.gh
Visit us: https://www.hsijournal.ug.edu.gh

significantly (F (5,54) = 10.56; p < 0.0001) the time spent in the target quadrant (probe trial, Figure 1C). Administration of MOE formulation improved escape time throughout the test days (Figure 1A), reduced total escape time (Figure 1B) and increased the time spent in the target quadrant when compared to the AlCl3 group (Figure 1C). The standard drug, donepezil (DPZ), also ameliorated the deficits induced by AlCl3 in the AD mice (Figure 1A, B, C). Interestingly, the improvement in learning and memory by MOE formulation and DPZ, as depicted by the MWM test, was similar to the vehicle group (VEH) with no AlCl3 AD induction.

Effects of optimised MOE formulation on AlCl3-induced AD mice by OF test.

The outcomes of the behavioural alterations evaluated in the OF test are illustrated in Figure 2. The AlCl3 AD mice showed a significant reduction (F (5,24) = 6.620; p = 0.0005) in the frequency of line crossing (Figure 2A) and time spent in the centre of the open field (F (5,24) = 4.867; p = 0.0033) (Figure 2B) when compared to the VEH group. However, there was no statistically significant difference (F (5,24) = 0.6312; p = 0.6778) observed in grooming frequency when compared to the VEH group (Figure 2C). In contrast, MOE formulation (10, 30, 100 mg/kg) or DPZ

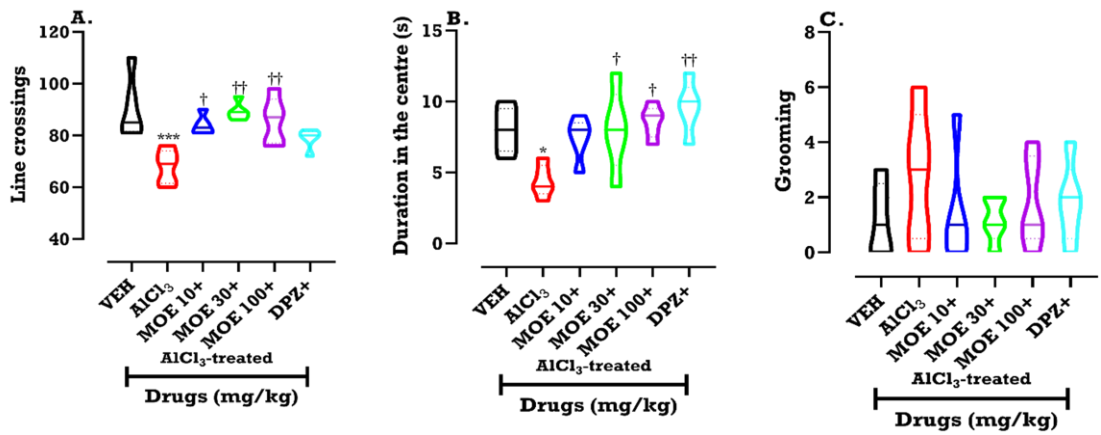

Figure 2. Effect of the optimized *M. oppositifolius* formulation on $AlCl_3$-induced AD-like dementia in the open field (OF) test: (A) frequency of line crossings, (B) time in center area and (C) grooming frequency. Data were presented as mean ± SEM. ***p < 0.001, *p < 0.05, compared to Vehicle-control group; ††p < 0.01, †p < 0.05, compared to disease-control ($AlCl_3$) group using one way ANOVA followed by Tukey's post-hoc test.

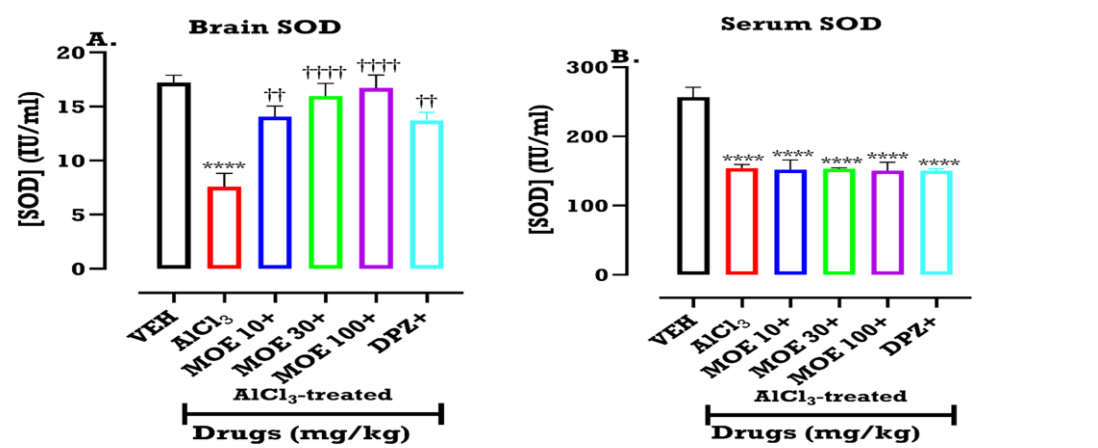

Figure 3. $AlCl_3$ induction and optimized formulation of MOE treatment effect on brain and serum SOD: (A) Brain SOD, (B) Serum SOD. Data were presented as mean ± SEM. ****p < 0.0001; significantly different form vehicle–control group: (One way ANOVA follow by Tukey's pot-hoc test). Significantly different from disease-control ($AlCl_3$) group: ††††p < 0.0001, ††p < 0.01: (One way ANOVA followed by Tukey's post-hoc test).

share
Send us an email: hsijournal@ug.edu.gh
Visit us: https://www.hsijournal.ug.edu.gh

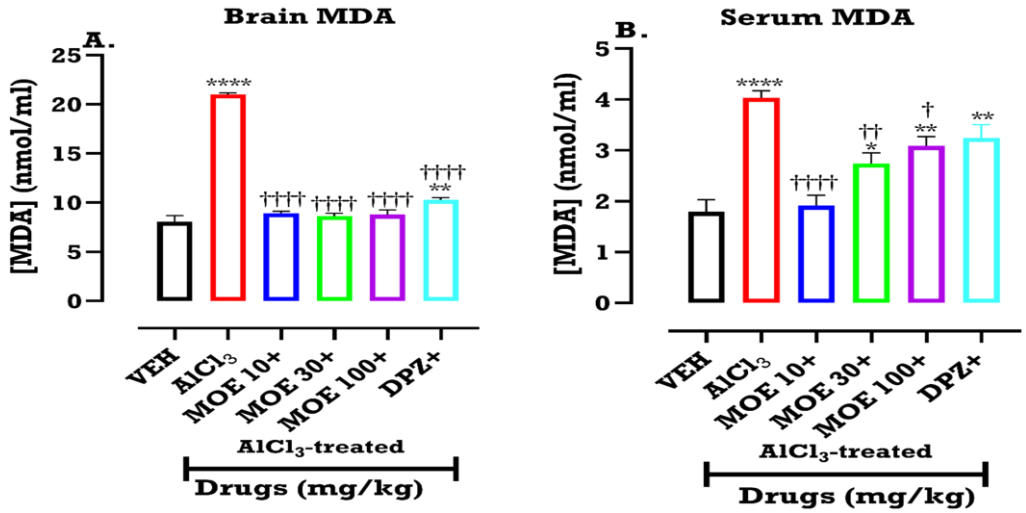

Figure 4. $AlCl_3$ induction and optimized formulation of MOE treatment effect on brain and serum MDA: (A) Brain MDA, (B) Serum MDA. Data were presented as mean ± SEM. ****p < 0.0001, **p < 0.01; significantly different form vehicle–control group: (One way ANOVA follow by Tukey's pot-hoc test). Significantly different from disease-control ($AlCl_3$) group: ††††p < 0.0001, ††p < 0.01, †p < 0.05: (One way ANOVA followed by Tukey's post-hoc test).

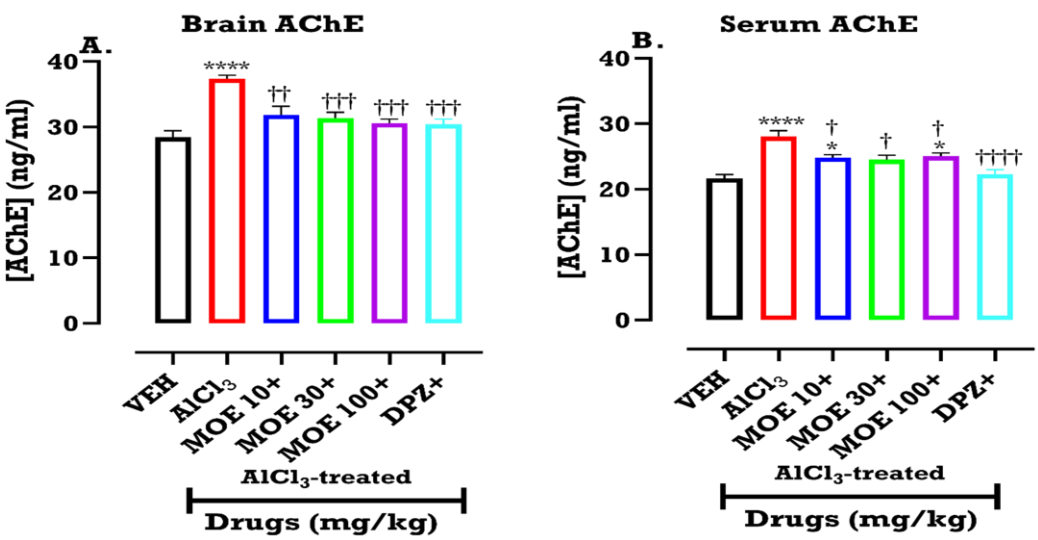

Figure 5. $AlCl_3$ induction and optimized formulation of MOE treatment effect on brain and serum AChE: (A) Brain AChE, (B) Serum AChE. Data were presented as mean ± SEM. ****p < 0.0001, *p < 0.05; significantly different form vehicle–control group: (One way ANOVA follow by Tukey's pot-hoc test). Significantly different from disease-control ($AlCl_3$) group: ††††p < 0.0001, ††p < 0.01, †p < 0.05: (One way ANOVA followed by Tukey's post-hoc test).

share
Send us an email: hsijournal@ug.edu.gh
Visit us: https://www.hsijournal.ug.edu.gh

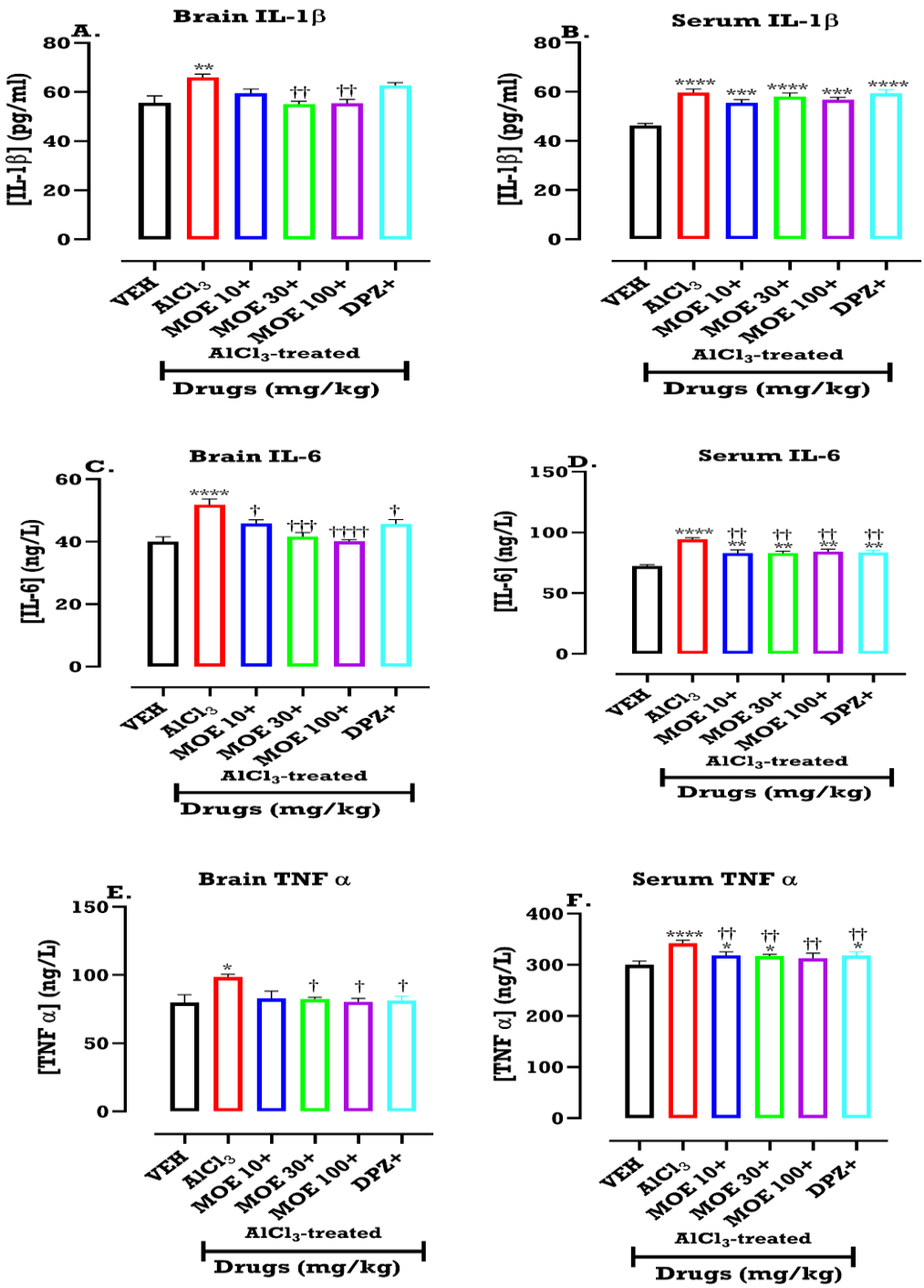

Figure 6. $AlCl_3$ induction and optimised formulation of MOE treatment effects on brain neurochemicals: (A) Brain IL-1β, (B) Serum IL-1β, (C) Brain IL-6, (D) Serum IL-6, (E) Brain TNF-α, (F) Serum TNF-α. Data were presented as mean ± SEM. ****p < 0.0001, ***p < 0.001, **p < 0.01, *p < 0.05; significantly different from vehicle–control group: (One way ANOVA followed by Tukey's post hoc test). Significantly different from disease-control ($AlCl_3$) group: ††††p < 0.0001, †††p < 0.001, ††p < 0.01, †p < 0.05: (One way ANOVA followed by Tukey's post-hoc test).

share
Send us an email: hsijournal@ug.edu.gh
Visit us: https://www.hsijournal.ug.edu.gh

administration to the AlCl3-induced AD mice significantly increased ($p < 0.05$) the frequency of line crossing (Figure 2A) and time spent in the centre square (Figure 2B), but not the grooming frequency when compared to the AlCl3 group (Figure 2C). The concentrations of the antioxidant SOD associated with AD pathology in the brain tissues and serum of mice are illustrated in Figure 3A and B, respectively. Brain and serum SOD were significantly decreased ($F (5, 30) = 11.86$; $p < 0.0001$); ($F (5,18) = 18.83$; $p < 0.0001$) in AlCl3-induced AD mice compared to the vehicle control group (Figure 3A and B, respectively). Conversely, MOE formulation (10, 30, and 100 mg/kg) and DZP (3 mg/kg) reversed ($p < 0.05$) the decrease in brain SOD concentration caused by $AlCl_3$ (Figure 3A). Unlike the brain SOD concentrations, MOE formulation and DPZ failed to reverse the $AlCl_3$-induced decrease in serum SOD (Figure 3B).

Effect of MOE formulation on brain tissue and serum concentration of MDA in $AlCl_3$-induced AD mice.

The oxidative stress marker, MDA, frequently observed in AD pathological findings was significantly elevated ($F (5, 30) = 182.4$; $p < 0.0001$); ($F (5, 18) = 16.59$; $p < 0.0001$) respectively by $AlCl_3$ in both the brain tissues and serum when compared to the vehicle control group (Figure 4A, B). In contrast, MOE formulation (10, 30, 100 mg/kg) just as DZP (3mg/kg) reversed ($p < 0.05$) the $AlCl_3$-associated increase in brain and serum MDA. Interestingly, MOE but not DZP reduced the brain MDA concentration to a level similar to vehicle control. In serum, however, both MOE formulation and DZP failed to reverse the MDA concentration to the vehicle control state (Figure 5B).

Effect of MOE formulation on brain tissue and serum content of AChE in $AlCl_3$-induced AD mice

AChE concentrations in brain tissue and serum were significantly elevated ($F (5, 30) = 11.29$; $p < 0.0001$); ($F (5, 18) = 12.45$; $p < 0.0001$) in the $AlCl_3$-induced AD mice compared to the vehicle control group (Figure 5A, B). Treatment with MOE formulation (10, 30, 100 mg/kg) and DZP (3 mg/kg) significantly reversed ($p < 0.05$) the $AlCl_3$-induced increase in both brain and serum AChE concentrations (Figure 5A, B). It is worth noting that the effect of MOE formulation on brain AChE was comparable to DPZ, the reference drug, and similar to the vehicle control group. However, the effect of MOE formulation on serum AChE was slightly lower compared to DPZ.

Effect of MOE formulation on brain tissue and serum cytokines (IL-1β, IL-6 and TNF-α) in $AlCl_3$-induced AD mice.

The concentrations of IL-1β, IL-6, and TNF-α in brain tissue were all significantly increased respectively ($F (5, 30) = 6.937$; $p = 0.0002$); ($F (5, 30) = 11.44$; $p < 0.0001$); ($F (5, 30) = 3.722$; $p = 0.0097$) in AD mice induced by $AlCl_3$ (Figure 6A, C, E). Treatment with 10 mg/kg MOE formulation significantly reduced the level of IL-6 (Figure 6C), but not IL-1β and TNF-α (Figure 6A, E). Both 30 and 100 mg/kg formulation of MOE treatment significantly decreased the IL-1β, IL-6 and TNF-α concentration. The reference drug, donepezil (3 mg/kg) treatment, significantly reduced the concentration of IL-6 and TNF-α (Figure 6C, E). Serum contents of the inflammation-related markers, IL-1β, IL-6, and TNF-α, in $AlCl_3$-induced AD mice were significantly elevated ($F (5, 18) = 15.73$; $p < 0.0001$); ($F (5,$

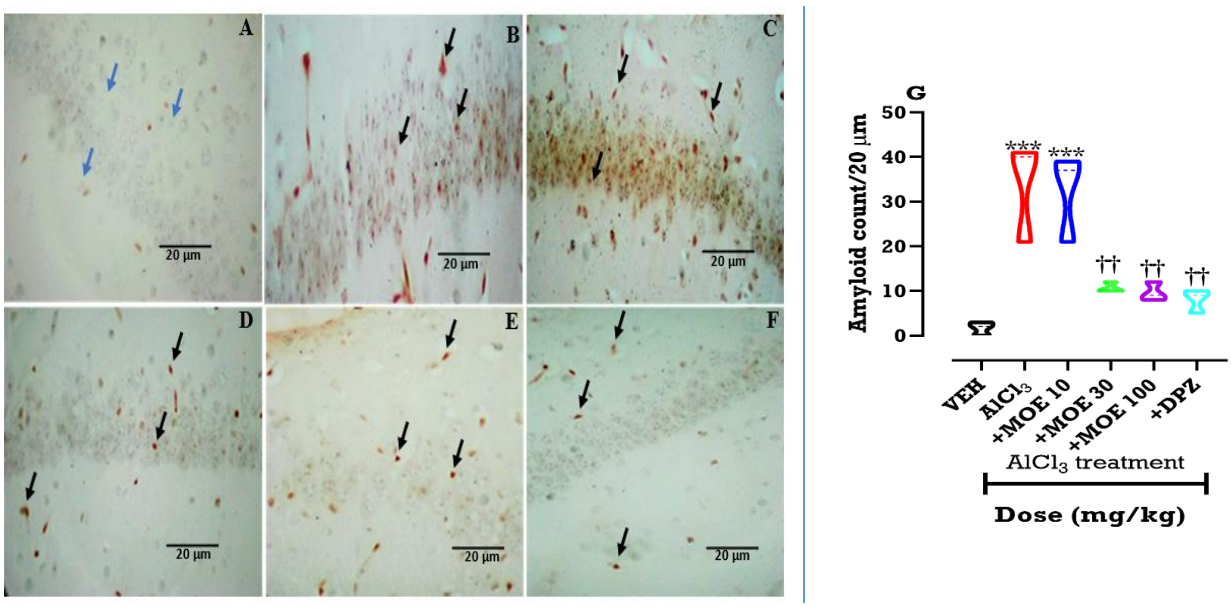

Figure 7. Effects of optimized *M. oppositifolius* formulation on Congo red staining of the hippocampus CA1 (400×) displayed as micrographs (left) and its amyloids quantification (right).

18) = 16.62; p < 0.0001), (F (5, 18) = 14.96; p < 0.0001) when compared to vehicle control group respectively (Figure 6B, D, F). Treatment with all three doses (10, 30, 100 mg/kg) of *M. oppositifolius* significantly decreased (p < 0.05) the concentrations of IL-6 and TNF-α (Figure 6D, F), but not IL-1β (Figure 6B), when compared to the diseased group. Treatment with the standard drug donepezil (3mg/Kg) also significantly reduced (p < 0.05) the concentrations of IL-6 and TNF-α (Figure 6D, F), but not IL-1β when compared to the diseased group (Figure 6B).

Effects of MOE formulation on Congo red-stained CA1 regions of the hippocampus

The Congo red-stained CA1 regions of the hippocampus in the control and treated groups are shown in Figure 7. The hippocampus of the vehicle control group shows typical, with almost no amyloid deposition (blue arrow) (Figure 7A). The disease control ($AlCl_3$) group had the most amyloid aggregation, indicated as a black arrow (Figure 7B). There was no decrease in amyloid deposition in the MOE formulation (10 mg/kg) treatment group, as observed and quantified in the micrograph (Figure 7C). Both 30 and 100 mg/kg formulation of MOE treatment decreased amyloid deposition considerably (Figure 7D, E). The standard drug, donepezil, also greatly reduced the number of amyloids observed in the micrograph (Figure 5F). Data from amyloid quantification are presented as mean ± SEM. ***p < 0.001; significantly different from vehicle–control group: (One-way ANOVA followed by Tukey's post hoc test). Significantly different from disease-control ($AlCl_3$) group: ††p < 0.01: (One way ANOVA followed by Tukey's post-hoc test). (A) Vehicle control: showing normal histology (blue arrow), (B) Disease control ($AlCl_3$ group): showing β-amyloid deposition (black arrow), (C) *M. oppositifolius* (MOE 10 mg/kg group): showing β-amyloid deposition similar to disease control group (black arrow), (D) *M. oppositifolius* (MOE 30 mg/kg group): showing reduced β-amyloid deposition (black arrow), (E) *M. oppositifolius* (MOE 100 mg/kg group): showing reduced β-amyloid deposition (black arrow), (F) Donepezil (DZP 3 mg/kg group): showing reduced β-amyloid deposition (black arrow) in the hippocampus.

DISCUSSION

This study evaluated an optimised formulation of *M. oppositifolius* leaf extract (MOE) in an $AlCl_3$-induced mouse model of Alzheimer's disease-like dementia. The study utilised chitosan and pectin to incorporate *M. oppositifolius* leaf extract into modified-release formulations in order to optimise its CNS effect. Modified-release drug delivery approaches are designed to meet specific clinical goals by adjusting drug release rates and sites while providing benefits that include better efficacy, fewer side effects, ease of use, and compliance among patients [29]. Herein, we report that MOE formulation reversed $AlCl_3$-associated cognitive deficits, neuro-inflammation, anxiogenic behaviour, impaired locomotion, and oxidative stress. In addition, MOE formulation reduced beta-amyloid deposition while preserving hippocampal neurons from degeneration. Dementia, which is characterised by learning and memory impairment, is one of the central features of AD [30,31,32]. This study used the Morris water maze (MWM) test to assess hippocampally dependent spatial learning and memory performance. Escape latency (i.e. the time required to locate the hidden platform) and probe trial (i.e. active exploration of the quadrant where the secret platform was previously positioned) were used to assess mouse spatial learning and memory retention. Here, we show that MOE formulation reversed the $AlCl_3$-associated decline in spatial learning by reducing the time it took for mice to find the platform.

In addition, MOE-treated mice performed better in the probe trial, suggesting that it was able to attenuate the $AlCl_3$-induced decline in memory retention. Consistent with our findings, previous studies with $AlCl_3$ have reported a marked decrease in spatial learning and probe trial memory performance in the MWM test [25,33]. The dentate gyrus (DG), CA3 and CA1 areas of the hippocampus are crucial in short-term and episodic learning and memory [34]. For instance, the ablation of granule cells in the DG caused deficits in spatial learning [35]. Also, inhibitory interneurons and excitatory pyramidal neurons in the CA1 region contribute to the regulation of spatial learning [36]. Since $AlCl_3$ causes neurodegeneration of several hippocampal regions with accompanying learning and memory deficits [25], MOE's ability to attenuate $AlCl_3$'s effect may suggest possible neurogenesis in the hippocampus. Though this assertion is yet to be proven, several lines of evidence have linked MOE's neuroactive effect to serotonin and brain-derived neuroprotective factor (BDNF), which are known to play pivotal roles in neurogenesis [37,13]. For instance, a study has proven that MOE improves depression-related aggressive behaviour in mice by increasing 5-HT levels and dendritic spine density in the prefrontal cortex [13]. Apart from this, various neurotransmitter imbalances, particularly acetylcholine (ACh), contribute to AD [38]. ACh is instrumental in learning and memory; thus, its hydrolysis by acetylcholinesterase (AChE) may cause learning and memory impairment. Indeed, ACh deficiency has been associated with AD-related dementia [39]. One of the mechanisms by which $AlCl_3$ causes memory impairment is via elevation in AChE activity, which leads to ACh deficiency [40]. In this study, MOE formulation reversed the $AlCl_3$-related increase in ACh, suggesting that the action of MOE formulation in improving learning and memory may be related to increased cholinergic neurotransmission.

Studies show a positive correlation between AD and anxiety behaviour as well as motor impairment [41,42]. In this study, mice exposed to $AlCl_3$ exhibited anxiety-like behaviour and reduced locomotor activity in the open field test. Consistent with previous reports where MOE improved anxiety behaviour and locomotor activity in the open field test, MOE formulation reversed the deficits

share
Send us an email: hsijournal@ug.edu.gh
Visit us: https://www.hsijournal.ug.edu.gh

induced by $AlCl_3$ [14,13]. The anxiolytic effect of MOE may be due to its GABA-enhancing effect previously reported by our lab [11]. Neuroinflammation, characterised by increased IL-1β, IL-6, and TNF-α, contributes to the onset and progression of AD [44]. These cytokines compromise neurogenesis and cause dysfunction in the neurotrophic system [45]. $AlCl_3$-induced AD promotes neuroinflammation through persistent activation of microglia, which releases IL-1β, IL-6, and TNF-α. The actions of these cytokines further contribute to beta-amyloid deposition, a primary feature of AD.

In our study, MOE formulation significantly reversed the $AlCl_3$-induced increase of IL-1β, IL-6, and TNF-α in the brain. In the serum, however, MOE formulation significantly reduced the IL-6 and TNF-α levels but not IL-1β. These findings suggest that MOE may reduce inflammation both peripherally and centrally. Indeed, previous studies reported that MOE exhibited an anti-inflammatory effect in carrageenan-induced paw oedema [46] and decreased activated microglia count in a lipopolysaccharide-induced neuroinflammation model [14]. Thus, the findings in this current study may suggest decreased microglial activation, as previously reported. The inception of AD is characterised by the build-up and clustering of beta-amyloid (Aβ) peptides, which may be occasioned by either an excess production or disruptions in the clearance mechanism [47]. Congo red staining techniques established that $AlCl_3$ induced the deposition of Aβ peptides in the hippocampus.

Conversely, MOE-treated mice displayed reduced neurodegeneration and exhibited minimal β-amyloid deposition, suggesting a protective effect against $AlCl_3$-induced neurotoxicity in mice [48,25]. Furthermore, the MOE-associated reduction in Aβ peptides in the hippocampus may further support the assertion that MOE reduces pathological activation of microglia in a manner that inhibits the release of pro-inflammatory cytokines and their involvement in amyloid formation and deposition [14]. A deficient antioxidant defence system in the brain leads to disequilibrium in initiating and eliminating reactive oxygen species, disruption of cellular pathways and lipid peroxidation. Similarly, oxidative stress is recognised as a significant etiological factor for the gradual deterioration of cognitive, memory, and motor functions [49]. Upon traversing the blood-brain barrier, aluminium promotes the generation of free radicals, which in turn impair mitochondrial function across various brain regions and cause neurodegeneration [50].

In the context of this study, MOE increased the antioxidant enzyme SOD in the brain tissue, while MDA, an indicator of lipid peroxidation, was significantly decreased in the serum and brain. The MDA result is consistent with a previous study that observed the anti-peroxidative effect of MOE in the liver [46]. In contrast, MOE failed to reverse the effect of $AlCl_3$ on serum SOD. The apparent discrepancy in serum SOD levels when compared to the study by [51] may be due to differences in solvent for extraction, impact of *in vivo* versus *in vitro* conditions, and differences in doses and species (mice versus rats) used.

Study limitation

The study was conducted on an animal model (mice) of AD induced by $AlCl_3$. This model may not fully represent AD pathology in humans. This limits the direct applicability of the results to human patients. With just six groups (n = 10) of mice, the sample size may be limited for detecting smaller but possibly significant effects of the treatment. Moreover, the duration of the study may not capture long-term outcomes or delayed effects of the optimised MOE formulation. The study concentrated on specific biomarkers such as SOD, MDA, AChE, and pro-inflammatory cytokines. However, it did not assess other crucial AD markers, such as p-tau or glutathione levels, which could have provided a more complete picture of the treatment's effects.

Future Research

The extract should be evaluated further by measuring other AD markers like Aβ, phosphorylated-tau, reduced glutathione (GSH), and catalase. Future research should also consider measuring other antioxidant markers such as glutathione S transferase, glutathione peroxidase and glutathione reductase associated with AlCl3-induced neurotoxicity. The neuroprotective effect of the extract should be further investigated in animal models that replicate human AD pathology using transgenic models. The optimised formulation used chitosan and pectin as carriers to enhance CNS delivery. While this method showed effectiveness in mice, further research is needed to evaluate whether these carriers would perform similarly in humans, especially regarding the permeability of the blood brain barrier (BBB)

Conclusion

The research findings suggest that an optimised formulation of *M. oppositifolius* improves learning and memory impairment and reduces anxiety-like behaviour, oxidative stress, and neuroinflammation in $AlCl_3$ model of Alzheimer's disease. The formulation also reduced Aβ peptide deposition in the CA1 region of the hippocampus of mice.

DECLARATIONS

Ethical consideration

Ethical approval was obtained from the Ghana Health Service Ethics Review Committee (GHS-ERC: 007/05/24).

Consent to publish

All authors agreed on the content of the final paper.

Funding

None

Competing Interest

The authors declare no conflict of interest

share
Send us an email: hsijournal@ug.edu.gh
Visit us: https://www.hsijournal.ug.edu.gh

Author contribution

KKEK and OAD conceptualised the research. JTP, KKEK, OAD, EKO, and KKAO conducted methodology and research investigations. JTP, KKEK, OAD, EKO, KKAO, PA, and DWA conducted data collection and analysis, manuscript writing, review, and editing. All authors read and approved the final manuscript.

Acknowledgement

We thank the Regional Director of Health Services for invaluable support throughout the study, the medical superintendent of Kade Government Hospital for facilitating data collection, and the labour suite staff for their assistance and support.

Availability of data

Data is available upon request to the corresponding author

REFERENCES

1. Moradi ZS, Momtaz S, Bayrami Z, Farzaei MH, Abdollahi M (2020) Nanoformulations of herbal extracts in treatment of neurodegenerative disorders. Front Bioeng Biotechnol 2020:1–4
2. Hussain G, Rasul A, Anwar H, Aziz N, Razzaq A, Wei W, Ali M, Li J, Li X (2018) Role of plant derived alkaloids and their mechanism in neurodegenerative disorders. Int J Biol Sci 2018:1
3. Villemagne VL, Burnham S, Bourgeat P, Brown B, Ellis KA, Salvado O, Szoeke C, Macaulay LS, Martins R, Maruff P, Ames D, Rowe CC, Masters CL (2013) Amyloid β deposition, neurodegeneration, and cognitive decline in sporadic Alzheimer's disease: a prospective cohort study. Lancet Neurol 4:357–367
4. Jack CR, Bennett DA, Blennow K, Carrillo MC, Dunn B (2018) NIA-AA research framework: Toward a biological definition of Alzheimer's disease. Alzheimers Dement 14(4):535–562
5. Tarragon E, Lopez D, Estrada C, Ana GC, Schenker E, Pifferi F, Bordet RJC, Herrero MT (2013) Octodon degus: A model for the cognitive impairment associated with Alzheimer's disease. CNS Neurosci Ther 19:643–648
6. Mahdi O, Baharuldin MTH, Nor NHM, Chiroma SM, Jagadeesan S, Moklas MAM (2019) Chemicals used for the induction of Alzheimer's disease-like cognitive dysfunctions in rodents. Biomed Res Ther 6(11):3460–3484
7. Kandimalla R, Reddy H (2016) Multiple faces of dynamin-related protein 1 and its role in Alzheimer's disease pathogenesis. Biochim Biophys Acta 1862(4):814–828
8. Nair RR, Corrochano S, Gasco S, Tibbit C, Thompson D, Maduro C, Ali Z, Fratta P, Arozena AAA, Cunningham TJ, Fisher EMC (2019) Uses for humanised mouse models in precision medicine. Mamm Genome 2019:1–3
9. Tiwari S, Atluri V, Kaushik KA, Yndart A, Nair M (2019) Alzheimer's disease: Pathogenesis, diagnostics, and therapeutics. Int J Nanomed 14:5541–5554
10. Kukuia KKE, Ameyaw EO, Mante PK, Adongo D, Woode E (2012) Screening of central effects of the leaves of *Mallotus oppositifolius* (Geiseler) Müll. Arg. in mice. Pharmacologia 688–689
11. Kukuia KK, Ameyaw EO, Woode E, Mante PK, Adongo DW (2016) Scientific evidence of plant with a rapid-onset and sustained antidepressant effect in a chronic model of depression: *Mallotus oppositifolius*. J Basic Clin Physiol Pharmacol 2016:3
12. Nwaehujor O, Ezeigbo II, Nwinyi FC (2013) Evaluation of *Mallotus oppositifolius* methanol leaf extract on the glycaemia and lipid peroxidation in alloxan-induced diabetic rats: A preliminary study. Biochem Res Int 2013:1–6
13. Kukuia KK, Appiah F, Dugbartey GJ, Takyi YF, Amoateng P, Amponsah SK, Adi-Dako O, Koomson AE, Aye F (2022) Extract of *Mallotus oppositifolius* (Geiseler) Müll. Arg. increased prefrontal cortex dendritic spine density and serotonin and attenuated para-chlorophenylalanine-aggravated aggressive and depressive behaviors in mice. Front Pharmacol 13
14. Kukuia K, Takyi F, Dugbartey G et al. (2023) Decreased hippocampal microglial cell activation by methanolic extract from the leaves of *Mallotus oppositifolius* (Geiseler) Müll. Arg contributes to its antidepressant-like effect. Mol Psychol 2(2)
15. Saeed N, El-Demerdash E, Abdel-Rahman H, Algandaby M, Al-Abbasi F, Abdel-Naim A (2012) Anti-inflammatory activity of methyl palmitate and ethyl palmitate in different experimental rat models. Toxicol Appl Pharmacol 264(1):84–93
16. Ye S, Jun Z, Huang J, Chen L, Yi L, Li X, Lv J, Miao J, Li H, Chen D, Li C (2021) Protective effect of Plastrum Testudinis extract on dopaminergic neurons in a Parkinson's disease model through DNMT1 nuclear translocation and SNCA's methylation. Biomed Pharmacother 141:111832
17. Rahman HS, Othman HH, Alitheen NB (2020) Novel drug delivery systems for loading of natural plant extracts and their biomedical applications. Int J Nanomedicine 15:2439–2483
18. Harun SN, Nordin SA, Gani SS, Shamsuddin AF, Basri M, Basri HB (2018) Development of nanoemulsion for efficient brain parenteral delivery of cefuroxime: designs, characterisations, and pharmacokinetics. Int J Nanomedicine 13:2571–2584
19. Tajes M, Ramos-Fernandez E, Weng-Jiang X, Bosch-Morato M, Guivernau B, Eraso-Pichot A, Salvador B, Fernández-Busquets X, Roquer J, Muñoz FJ (2014) The blood-brain barrier: structure, function and therapeutic approaches to cross it. Mol Membr Biol 31:152–167
20. Zhao D, Yu S, Sun B, Guo SS, Zhao K (2018) Biomedical applications of chitosan and its derivative nanoparticles. Polym (Basel) 10:1
21. Adi-Dako O, Ofori-Kwakye K, Frimpong-Manso S, Boakye-Gyasi M, Sasu C, Pobee M (2016) Physicochemical and antimicrobial properties of cocoa pod husk pectin intended as a versatile pharmaceutical excipient and nutraceutical. J Pharmaceutics
22. Amponsah S, Yeboah S, Kukuia K, N'guessan B, Adi-Dako OA (2021) Pharmacokinetic evaluation of a pectin-based oral multiparticulate matrix carrier of carbamazepine. Adv Pharmacol Pharm Sci 2021
23. Adi-Dako O, Ofori-Kwakye K, Amponsah BI, Kuntworbe OE (2018) Potential of cocoa pod husk pectin-based

modified release capsules as a carrier for chronodelivery of hydrocortisone in Sprague-Dawley rats. J Drug Deliv

24. Imbeah E, Adi-Dako O, N'guessan B, Kukuia K, Dankyi B, Adams I, Ofori-Attah E, Appiah-Opong R, Amponsah S (2022) Pharmaceutical and pharmacokinetic evaluation of a newly formulated multiparticulate matrix of levodopa and carbidopa. ADMET DMPK 11:97–115

25. Chen X, Zhang M, Ahmed M, Surapaneni KM, Veeraraghavan VP, Arulselvan P (2021) Neuroprotective effects of ononin against the aluminium chloride-induced Alzheimer's disease in rats. Saudi J Biol Sci 28:4232–4239

26. Bromley-Brits K, Deng Y, Song W (2011) Morris water maze test for learning and memory deficits in Alzheimer's disease model mice. J Vis Exp 53:1–5

27. Prut L, Belzung C (2003) The open field as a paradigm to measure the effects of drugs on anxiety-like behaviors: a review. Eur J Pharmacol 463:3–33

28. García-Ayllón MS, Small DH, Avila J, Sáez-Valero J (2011) Revisiting the role of acetylcholinesterase in Alzheimer's disease: cross-talk with P-tau and β-amyloid. Front Mol Neurosci 4:22

29. Revel J, Gorria P (2019) Modified-release formulations: improving efficacy and patient compliance. Solid Dosage Drug Dev Manuf Suppl 2019:6–8

30. Sakimoto Y, Oo PM, Goshima M, Kanehisa I, Tsukada Y, Mitsushima D (2021) Significance of GABAA receptor for cognitive function and hippocampal pathology. Int J Mol Sci 22:22

31. Cieślik P, Borska M, Wierońska JM (2023) A comparative study of the impact of NO-related agents on MK-801- or scopolamine-induced cognitive impairments in the Morris water maze. Brain Sci 13:410

32. Twarowsk B, Herbet M (2023) Inflammatory processes in Alzheimer's disease—pathomechanism, diagnosis and treatment: a review. Int J Mol Sci 24:6518

33. Inwang UA, Ekong DKGBM, Obasi CP, Onyebuenyi M, Nwaji AR (2023) The anti-oxidative and cognitive properties of Zingiber officinale rhizome ethanol extract and its dichloromethane and n-hexane fractions against aluminum chloride-induced neurotoxicity in Swiss mice

34. Meier K, Merseburg A, Isbrandt D, Marguet SL, Morellini F (2020) Dentate gyrus sharp waves, a local field potential correlate of learning in the dentate gyrus of mice. J Neurosci 40:7105–7118

35. Garthe A, Kempermann G (2013) An old test for new neurons: refining the Morris water maze to study the functional relevance of adult hippocampal neurogenesis. Front Neurosci 7:63

36. Jeong N, Singer A (2022) Learning from inhibition: functional roles of hippocampal CA1 inhibition in spatial learning and memory. Curr Opin Neurobiol 76

37. Begyinah RK, Adutwum-Ofosu KK, Mensah JA, Kwapong AA, Appiah F, Burns FB, Amoateng P, Kukuia KKE (2024) Elevated brain-derived neurotrophic factor levels and preserved hippocampal dendritic spine density underlie the rapid-onset antidepressant effect of extracts from *Mallotus oppositifolius*. IBRO Neurosci Rep

38. Loewenstein D, Acevedo A, Luis C, Crum T, Barker W, Duara R (2004) Semantic interference deficits and the detection of mild Alzheimer's disease and mild cognitive impairment without dementia. J Int Neuropsychol Soc 10:91–100

39. Liaquat L, Sadir S, Batool Z, Tabassum S, Shahzad S, Afzal A, Haider S (2019) Acute aluminum chloride toxicity revisited: study on DNA damage and histopathological, biochemical and neurochemical alterations in rat brain. 217:202–211

40. Elreedy HA, Elfiky A, Mahmoud A, Ebrahim KS, Ghazy M (2022) Effect of quercetin as therapeutic and protective agent in aluminum chloride-induced Alzheimer's disease rats. Egypt J Chem 65:633–641

41. Mendez M (2021) The relationship between anxiety and Alzheimer's disease. J Alzheimers Dis Rep 8:171–177

42. Pentkowski NS, Rogge-Obando KK, Donaldson TN, Bouquin SJ, Clark BJ (2021) Anxiety and Alzheimer's disease: behavioral analysis and neural basis in rodent models of Alzheimer's-related neuropathology. Neurosci Biobehav Rev 127:647–658

43. Kukuia KK, Ameyaw EO, Woode E, Mante PK, Adongo DW (2016) Scientific evidence of plant with a rapid-onset and sustained antidepressant effect in a chronic model of depression: Mallotus oppositifolius. J Basic Clin Physiol Pharmacol 3

44. Tian Z, Ji X, Liu J (2022) Neuroinflammation in vascular cognitive impairment and dementia: current evidence, advances, and prospects. Int J Mol Sci 23:6224

45. Gąssowska-Dobrowolska M, Chlubek M, Kolasa A, Tomasiak P, Korbecki J, Skowrońska K, Tarnowski M, Masztalewicz M, Baranowska-Bosiacka I (2023) Microglia and astroglia—The potential role in neuroinflammation induced by pre- and neonatal exposure to lead (Pb). Int J Mol Sci 24:9903

46. Nwaehujor CO, Ezeja MI, Udeh NE, Okoye OD, U R I (2014) Anti-inflammatory and antioxidant activities of Mallotus oppositifolius (Geisel) methanol leaf extracts. Arab J Chem 7:805–810

47. Sun X, Chen WD, Wang YD (2015) β-Amyloid: the key peptide in the pathogenesis of Alzheimer's disease. Front Pharmacol 6

48. Jadhav R, Kulkarni YA (2023) Effects of baicalein with memantine on aluminium chloride-induced neurotoxicity in Wistar rats. Front Pharmacol 14

49. Ali A, Shah T, Haider G, Awan MIGM, Munsif F, Ijaz A (2023) Strigolactone-mediated oxidative stress alleviation in Brassica rapa through upregulating antioxidant system under water deficit conditions. J Plant Growth Regul 42:4675–4687

50. Kumar V, Gill KD (2009) Aluminium neurotoxicity: neurobehavioural and oxidative aspects. Arch Toxicol 83:965–978

51. Onyeka IP, Onyegbule FA, Ezugwu CO, Ike CJ, Ikeotuonye CB (2021) Antioxidant potential of crude methanol leaf extract and fraction of *Mallotus oppositifolius*. J Complement Altern Med Res 16:168–184